then, if an overlap region exists, one obtains

$$\frac{U_\tau^2}{\nu} f' = \frac{\partial U}{\partial y} = \frac{U_N}{N} g' \tag{5}$$

within this region.

Since the right-hand side of this equation is independent of the kinematic viscosity ν, so must the left-hand side and $f' \sim 1/(yU_\tau/\nu)$. Thus, $g' \sim 1/(y/N)$ and one obtains

$$\frac{U}{|U_N|} = -A \ell n \left| \frac{y}{N} \right| - B \tag{6}$$

in this overlap region. For the data shown in Fig. 1, $A = 0.3$ and $B = 1.3$.

Clearly, Eq. (6) does not describe the $U/|U_N|$ vs y/N profile for $y/N > 0.2$. If another function (y/N) is added to Eq. (4), the $U/|U_N|$ can be forced to -1 at $y = N$. A candidate function is y/N since the outer region mean velocity profile $0.4 < y/\delta < 0.8$ appears to be very linear for the far downstream detached flow locations where $\gamma_{puw} \ll \frac{1}{2}$. Thus, we can write

$$\frac{U}{|U_N|} = A\left(\frac{y}{N} - \ell n \left| \frac{y}{N} \right| - 1 \right) - 1 \tag{7}$$

since this equation produces $U/|U_N| = -1$ and $\partial U/\partial y = 0$ at $y/N = 1$ and $B = 1 + A$. The term Ay/N contributes little to $U/|U_N|$ near the wall. The use of only one empirical constant A is a particularly striking feature of Eq. (7).

Figure 1 shows that Eq. (7) closely describes the mean velocity profile for $0.02 < y/N < 1.0$ with $A = 0.3$. It should be noted that experimental values of N are $\pm 15\%$ uncertain. For $y/N > 1$, the data at 3.53 m ($\gamma_{puw} = 0.33$) and 3.68 m ($\gamma_{puw} = 0.16$) and Westphal's data ($\gamma_{puw} = 0.02$) for a backward facing step are higher than Eq. (7). For 3.97 m ($\gamma_{puw} = 0.1$) and 4.34 m ($\gamma_{puw} = 0.06$) the data fall below Eq. (7).

For $y/N < 0.02$, Eq. (2) can be used to describe the velocity profile of the viscous wall layer and to estimate the mean surface shearing stress when C is determined at $y/N = 0.02$. For example, at 4.34 m, $P' = 120$ and $C_f/2 = 1 \times 10^{-4}$. This skin friction coefficient is about an order of magnitude smaller than upstream of detachment. For the 4.34 m data, $y/N = 0.02$ corresponds to $yU_\tau/\nu = 2.6$. This is a reasonable number in view of the viscous sublayer thickness for attached boundary layers, $yU_\tau/\nu \approx 5$.

Conclusions

Equation (7) can be used to describe the velocity profile of the middle region of the mean backflow, $0.02 < y/N < 1.0$, when $\gamma_{pu} < \frac{1}{2}$ near the wall. Laser anemometer and pulsed-wire anemometer data both support this mean velocity profile description. Nearer the wall, the viscous layer can be described by Eq. (2), although no experimental data in this region have been obtained. Farther away from the wall, $y/N > 1.0$, Eq. (7) does not describe the mean velocity profile well since this outer backflow region is influenced strongly by the large-scale outer region flow.

Equations (2) and (7) can be used as near wall backflow functions for separated flow calculation methods when $\gamma_{pu} < \frac{1}{2}$. Since these equations describe the portion of the mean backflow where $\partial U/\partial y \leq 0$, they eliminate the need for a calculation method to model the near wall flow where $\partial(-\overline{uv})/\partial y$ and $\partial U/\partial y$ are of opposite signs.

Acknowledgments

This work was done in conjunction with work supported by the Experimental Fluid Dynamics Branch of NASA Ames Research Center and work supported by the Office of Naval Research.

References

[1] Simpson, R. L., Chew, Y.-T., and Shivaprasad, B. G., "The Structure of a Separating Turbulent Boundary Layer. Part 1. Mean Flow and Reynolds Stress," *Journal of Fluid Mechanics*, Vol. 113, 1981, pp. 23-51.

[2] Simpson, R. L., Chew, Y.-T., and Shivaprasad, B. G., "The Structure of a Separating Turbulent Boundary Layer. Part 2. Higher-Order Turbulence Results," *Journal of Fluid Mechanics*, Vol. 113, 1981, pp. 53-73.

[3] Shiloh, K., Shivaprasad, B. G., and Simpson, R. L., "The Structure of a Separating Turbulent Boundary Layer. Part 3. Transverse Velocity Measurements," *Journal of Fluid Mechanics*, Vol. 113, 1981, pp. 75-90.

[4] Simpson, R. L., "A Review of Some Phenomena in Turbulent Flow Separation," *Journal of Fluids Engineering*, Vol. 103, 1981, pp. 520-533.

[5] Hastings, R. C., private communication, Royal Aircraft Establishment, Bedford, England, 1981.

[6] Westphal, R. V., "Experimental Study of a Reattaching Flow in a Sudden Expansion," Ph.D. Thesis, Dept. of Mechanical Engineering, Stanford University, 1982.

Upstream Influence in Sharp Fin-Induced Shock Wave Turbulent Boundary-Layer Interaction

D. S. Dolling* and S. M. Bogdonoff†
Princeton University, Princeton, New Jersey

Introduction

THREE-dimensional shock wave turbulent boundary-layer interactions are complex phenomena which occur in a wide variety of practical internal and external aerodynamic problems. Common examples are the sidewall interactions in engine inlets, and protuberance and fin-induced flowfields. Up until the last few years, most studies have been experimental. The recent rapid development of computational fluid dynamics has now made it possible to simulate numerically certain three-dimensional interactive flowfields, such as the skewed shock wave interaction.[1] Overall, good comparisons of numerical predictions with experiment have been obtained.

This flowfield has been the subject of many investigations, including the current study. The interaction is generated easily using the model configuration sketched in Fig. 1. It consists of an unswept, semi-infinite sharp fin at angle of attack α mounted normal to a flat surface on which the incoming boundary layer develops. A swept interaction is generated whose scale increases in the spanwise direction. Although much has been learned about this flowfield from such detailed experimental studies as those of Oskam et al.[2] and Peake,[3] many critical questions remain unanswered. One of the most fundamental is that of which parameters control the interaction scale and spanwise growth.

In an attempt to provide a partial answer to this question, measurements have been made of how a primary interaction length scale, namely, upstream influence, develops spanwise in this flowfield. Fin models have been tested at various α in

Received July 24, 1981; revision received May 6, 1982.

*Research Staff Member and Lecturer, Department of Mechanical and Aerospace Engineering. Member AIAA.

†Professor and Chairman, Department of Mechanical and Aerospace Engineering. Fellow AIAA.

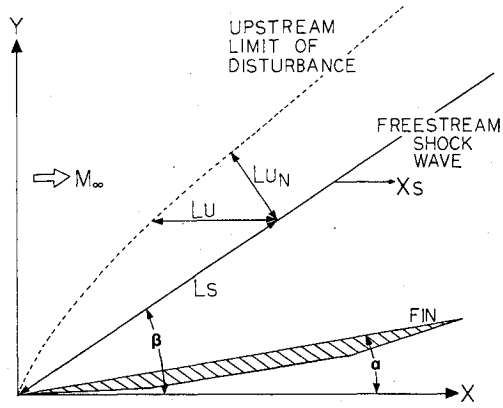

Fig. 1 Model configuration and definition of length scales.

several high Reynolds number, Mach 3 turbulent boundary layers. Results from this study are presented in this Note.

Test Program

The model geometry, the coordinate system, and relevant length scales are shown in Fig. 1. Two test surfaces were used. One was the tunnel floor and the other a sharp leading-edged, horizontal plate which spanned the tunnel. Both surfaces were instrumented with rows of pressure taps aligned with the X axis.

All tests were made in Princeton University's 20×20-cm blowdown tunnel under approximately adiabatic wall temperature conditions. The test Mach number M_∞ was 2.95. In the first test series, surface pressure distributions and streak patterns were obtained for $1\le\alpha\le14$ deg. The stagnation pressure was 6.8×10^5 Nm$^{-2}\pm1\%$, the stagnation temperature 265 K$\pm5\%$, and the nominal freestream Reynolds number Re_∞ was 6.3×10^7 m^{-1}. In the second set of tests, α was fixed at 8 deg and the same surface measurements made at $Re_\infty\sim12.6\times10^7$ m^{-1} and 18.9×10^7 m^{-1}.

The incoming boundary layers on both test surfaces are two dimensional, fully turbulent, and in equilibrium.[4] Boundary-layer trips were not used. At these high Reynolds numbers, transition on the flat plate occurred within 2 cm of the leading edge. The interaction region was of order 100 local boundary layer thicknesses downstream of this station.

Upstream Influence Estimation

L_u was estimated from wall pressure distributions and from kerosene-lampblack streak patterns. This surface flow visualization method, described in Appendix B of Ref. 5, has two major advantages over the conventional oil streak technique. First, no smearing of the trace occurs since the tunnel is not shut down until all the kerosene has evaporated. Second, the patterns are lifted directly off the surface on sheets of transparent tape, providing full scale, undistorted records. The repeatability is excellent.

The upstream limit of disturbed flow was measured from where the streaks are first deflected. This is subjective, but independent observers can consistently bracket L_u to within a few percent. At each test condition, comparisons were made with L_u estimated from wall pressures. In this case, the upstream limit is taken as being where the tangent to the initial pressure rise intersects the horizontal line representing the undisturbed pressure level. The two methods agree well. The worst agreement ($\pm5\%$) occurs for small α, where the initial pressure gradient is shallow and the streak turning angle small.

At the far boundary of the flowfield the fin shock wave interacts with the tunnel side-wall boundary layer, limiting the spanwise extent of interference-free flow. The extent of the interference region was clearly visible on the surface streak patterns and no measurements were made in or close to it.

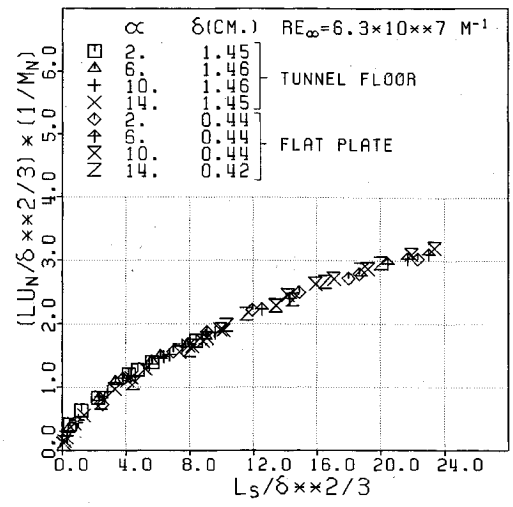

Fig. 2 Spanwise and streamwise upstream influence correlation at constant Reynolds number.

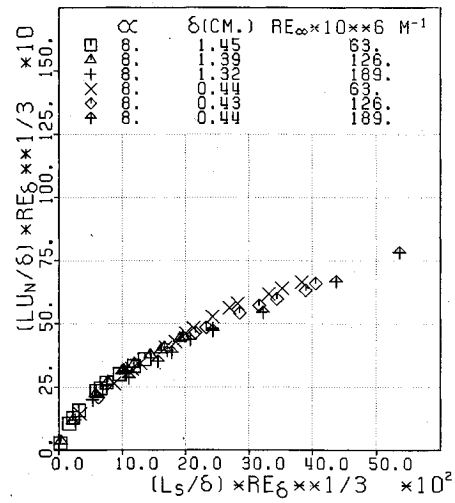

Fig. 3 Spanwise and streamwise upstream influence correlation at constant shock wave strength.

Results and Discussion

In Ref. 4, an upstream influence correlation method was developed for three-dimensional swept compression ramp interactions. The functional relationship for the streamwise and spanwise scaling was given in the form

$$\frac{L_u}{\delta}Re_\delta^a=f\left(\frac{z}{\delta}Re_\delta^b,\ \alpha_w,\ \lambda_w,\ M_\infty\right) \tag{1}$$

where α_w is the streamwise compression ramp angle, λ_w the corner line sweepback angle, and z the spanwise distance from the model apex measured normal to the undisturbed direction. At any spanwise station, δ is the undisturbed boundary-layer thickness just upstream of the interaction start. In a parametric experimental study at the same flow conditions as the present tests, good correlations were obtained with $a=b=1/3$.

The same approach, subject to the modifications given subsequently, has been applied to the present test data. For semi-infinite, unswept sharp fins, the only relevant geometric parameter is α. At a fixed M_∞, α determines the shock wave angle β, so α and β are not independent and, therefore, only one is needed. If β is chosen, it can be replaced by $M_\infty\sin\beta$ which introduces, as might be anticipated, the normal Mach number M_n. Thus, in the normal coordinate system of Fig. 1,

Eq. (1) can be rewritten as

$$\frac{L_{u_n}}{\delta} Re_\delta^a = f\left(\frac{L_s}{\delta} Re_\delta^b,\ M_n\right) \qquad (2)$$

for a fixed M_∞.

The test data confirm the validity of this functional relationship. Similar to the compression ramp studies, good correlations are obtained with $a=b=1/3$. Over the limited range of α tested, L_{u_n} was found to be weakly, but linearly, dependent on M_n. Large values of L_{u_n} were observed with very weak shock waves. Figure 2 shows results obtained in the first test series, carried out at constant Re_∞. In this case $Re_\delta^{1/3}$ can be written as $Re_\infty^{1/3}\delta^{1/3}$, so the appropriate correlating parameters are

$$\frac{L_{u_n}}{\delta^{2/3}} \frac{1}{M_n} \text{ vs } \frac{L_s}{\delta^{2/3}}$$

Note that Fig. 2 axes are $cm^{1/3}$. Results from the second test series, at variable Re_∞, but with α fixed at 8 deg, are shown in Fig. 3. Since M_n is fixed, the appropriate correlating parameters are

$$\frac{L_{u_n}}{\delta} Re_\delta^{1/3} \text{ vs } \frac{L_s}{\delta} Re_\delta^{1/3}$$

In both figures, the data correlate well.

The importance of M_n has been demonstrated by Stalker.[6] In an extension of Lighthill's small perturbation analysis[7] to infinite swept flows, Stalker showed it to be the dominant parameter controlling upstream influence. His experimental upstream influences (defined as the distance normal to the isobars over which the perturbation pressure increased by the factor e), measured in skewed shock wave and forward facing swept step interactions, at a fixed M_∞ (=2.36) and Re_∞, were in overall agreement with the analysis. The current data provide further evidence of the importance of M_n.

Concluding Remarks

The results described show that a scaling technique can be developed which correlates upstream influence in sharp fin-induced shock wave turbulent boundary-layer interactions. Although the dimensional scale differs from that in swept compression ramp flows at similar flow conditions, the scale effects of changing boundary-layer thickness and Reynolds number are the same. In both cases, the scale increases with increasing boundary-layer thickness and decreasing Reynolds number.

In applying these results, a word of caution is in order. Since the tests were made at a single Mach number and over a limited range of shock wave strengths, Reynolds numbers, and boundary layers, the possible general validity of the scaling law cannot be assessed. It is likely that the empirical constants are dependent on freestream conditions. As part of a continuing research program, tests at Mach 2 will be made shortly and hopefully they will answer these questions.

Acknowledgments

This work was supported by the U.S. Air Force Office of Scientific Research under Contract F49620-80-C-0092 monitored by Dr. J. Wilson. Discussions with Dr. G. S. Settles are gratefully acknowledged.

References

[1] Horstman, C. C. and Hung, C. M., "Computation of Three-Dimensional Turbulent Separated Flows at Supersonic Speeds," AIAA Paper 79-0002, Jan. 1979.

[2] Oskam, B., Bogdonoff, S. M., and Vas, I. E., "Study of Three-Dimensional Flow Fields Generated by the Interaction of a Skewed Shock Wave with a Turbulent Boundary Layer," AFFDL-TR-75-21, Feb. 1975.

[3] Peake, D. J., "The Three-Dimensional Interaction of a Swept Shock Wave with a Turbulent Boundary Layer and the Effects of Air Injection on Separation," Ph.D. Thesis, Carleton University, Ottawa, Canada, 1975.

[4] Settles, G. S., Perkins, J. J., and Bogdonoff, S. M., "Upstream Influence Scaling of 2D and 3D Shock/Turbulent Boundary Layer Interactions at Compression Corners," AIAA Paper 81-0334, Jan. 1981.

[5] Settles, G. S., "An Experimental Study of Compressible Turbulent Boundary Layer Separation at High Reynolds Numbers," Ph.D. Thesis, Princeton University, Princeton, N.J., 1975.

[6] Stalker, R. J., "Sweepback Effects in Turbulent Boundary Layer Shock Wave Interaction," *Journal of Aerospace Sciences*, Vol. 27, No. 5, 1960, pp. 348-356.

[7] Lighthill, M. J., "On Boundary Layers and Upstream Influence: Part II—Supersonic Flows without Separation," *Proceedings of the Royal Society*, A217, 1953, pp. 478-507.

A Comparative Study of Time-Marching and Space-Marching Numerical Methods

R.N. Gupta,* J.N. Moss,† and A.L. Simmonds‡
NASA Langley Research Center, Hampton, Virginia

Introduction

RECENTLY an evaluation[1] of the three different flowfield codes[2-4] for the Jupiter entry conditions was presented. However, direct comparisons have been hampered by the fact that the three codes use different solution procedures, different computational mesh sizes, different chemical and turbulence models, different convergence criterion, as well as a different number of computational grid points along and perpendicular to the body. Even for the only common feature of radiative transport code, there are subtle differences in the spectral details of some species. Thus, for an objective evaluation of the different numerical solution methods employed by these codes, it would be desirable to select a simple no-blowing perfect-gas flowfield case for which the turbulent models are well established. The purpose of this Note is to present the results of such a study.

Analysis

The results have been obtained by employing two of the three numerical codes mentioned earlier. The first of these two is a space-marching method (perfect-gas version of HYVIS[2]) that solves the steady-state viscous-shock-layer-type equations by the method of Davis.[5] The second one is a time-marching method (perfect-gas version of COLTS[3]) that employs the time-asymptotic, two-step, finite difference method of MacCormack[6] for the solution of time-dependent viscous-shock-layer-type equations. For this study, the two methods also employ the same turbulence model[7] with and without blowing.

In addition to the prescribed surface blowing rate distribution, the boundary conditions employed along the

Received Oct. 19, 1981; revision received May 3, 1982. This paper is declared a work of the U.S. Government and therefore is in the public domain.

*NRC-Senior Research Associate, Aerothermodynamics Branch, Space Systems Division; on leave from IIT, Kanpur, India; Professor, Department of Aeronautical Engineering. Member AIAA.

†Research Leader, Aerothermodynamics Branch, Space Systems Division. Member AIAA.

‡Mathematician, Aerothermodynamics Branch, Space Systems Division. Member AIAA.